


Review

Preparation, Properties, and Applications of Near Stoichiometric Lithium Tantalate Crystals

Xuefeng Xiao ^{1,2,*}, Jiashun Si ^{1,2}, Shuaijie Liang ^{1,2} , Qingyan Xu ^{1,2}, Huan Zhang ^{1,2}, Lingling Ma ^{1,2}, Cui Yang ^{1,2} and Xuefeng Zhang ^{1,3}

¹ Key Laboratory of Physics and Photoelectric Information Functional Materials Sciences and Technology, North Minzu University, Wenchang Road 204, Yinchuan 750021, China; sijias0121@163.com (J.S.); l120850384@163.com (S.L.); xuqingyan97@163.com (Q.X.); zhang_huan722@163.com (H.Z.); mall@nmu.edu.cn (L.M.); yangcui0712@126.com (C.Y.); zxf905@126.com (X.Z.)

² College of Electric and Information Engineering, North Minzu University, Wenchang Road 204, Yinchuan 750021, China

³ Ningxia Ju Jing Yuan Crystal Technology, Co., Ltd., Shahu Road 304, Shizuishan 753000, China

* Correspondence: xuefengxiao@nmu.edu.cn

Abstract: Lithium tantalate crystal is widely used in optical devices, infrared detectors and surface acoustic wave devices because of its excellent piezoelectric, acousto-optic and nonlinear optical properties. The Li content of near stoichiometric lithium tantalate (NSLT) crystal is higher than that of congruent lithium tantalate (CLT) crystal. Therefore, the performance of NSLT crystal is better than that of CLT crystal in some aspects. This article reviews the physical properties, preparation methods and current research status in acoustics and optics of NSLT crystals. It also looks forward to the improvement of NSLT crystal preparation methods and their applications in surface acoustic wave (SAW) filters and optics. With the increase of Li content, the acoustic performance of NSLT crystals is expected to be comprehensively improved, achieving the application of SAW filters in 5G communication.

Keywords: near stoichiometric lithium tantalate; physical property; optical application; acoustic application



Citation: Xiao, X.; Si, J.; Liang, S.; Xu, Q.; Zhang, H.; Ma, L.; Yang, C.; Zhang, X. Preparation, Properties, and Applications of Near Stoichiometric Lithium Tantalate Crystals. *Crystals* **2023**, *13*, 1031. <https://doi.org/10.3390/cryst13071031>

Academic Editor: Maria Dinescu

Received: 30 May 2023

Revised: 20 June 2023

Accepted: 26 June 2023

Published: 28 June 2023



Copyright: © 2023 by the authors. Licensee MDPI, Basel, Switzerland. This article is an open access article distributed under the terms and conditions of the Creative Commons Attribution (CC BY) license (<https://creativecommons.org/licenses/by/4.0/>).

1. Introduction

Lithium tantalate (LiTaO₃, LT) crystal has been widely used in the fields of acoustics and optics due to excellent electro-optic, non-linear optical [1,2], piezoelectric and pyroelectric properties [3]. At present, commercial LT crystals are mainly CLT crystals with Li:Ta = 48.5:51.5. A large number of defects appear due to the lack of Li in the CLT crystal, including Li vacancy defects (V_{Li}) [4], Ta inversion defects (Ta_{Li}) [5], etc. Li vacancy defects will increase the coercivity field in the crystal [6], and Ta_{Li} antiposition defects (Ta at Li site) will cause optical damage effects [7]. Therefore, how to reduce the internal defects of LT crystals has become a hot research topic.

There are two ways to reduce the internal defects of crystals. One is doping with other ions [8], such as Fe and Mg. The other way is growing NSLT crystals with Li: Ta = 1:1, which has lower coercive field, lower refractive index and higher Curie temperature [9,10]. Therefore, it is necessary to study the growth of NSLT crystals.

LT crystal has been applied in SAW filters. With the advent of the 5G era, the performance of traditional filters cannot meet the market demand, so we must improve the performance of SAW filters from the material or technology aspect. In terms of materials, it is necessary to improve the electromechanical coupling coefficient (K²), and reduce the temperature drift coefficient (TCF) and insertion loss. Because the NSLT has better optical properties and higher sensitivity [11], it can be used as an optical information storage material and laser frequency doubling material [12]. Therefore, NSLT crystal has great

application prospects in acoustics and optics. Based on this, this paper reviews the physical properties, growth methods, and applications in optics and acoustics of NSLT crystals and looks forward to the research and application hot spots of NSLT crystals. It is expected that NSLT crystals will meet the application of SAW filter devices in the future.

2. Physical Properties of Crystals

At present, the commonly used crystal is CLT crystal with Li:Ta = 48.5:51.5. Due to the lack of lithium, a large number of defects appear in LT crystals, including Li vacancies and Ta_{Li} antiposition [13] defects. In order to reduce the internal defects, Katz proposed the NSLT crystal with Li:Ta close to 1:1, and the phase diagram is shown in Figure 1. It can be seen from the phase diagram that the Curie temperature of the crystal is different when the content of Li is different [14].

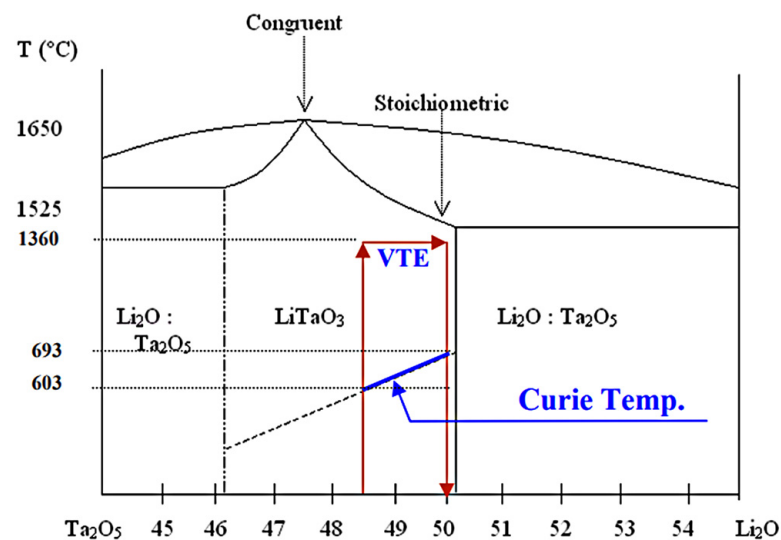


Figure 1. Phase diagram of LT crystal [14].

Shi et al. [15,16] found through analysis of the Raman and OH⁻ absorption spectra of CLT and NSLT crystals, which, as the Li content in the crystal increases, the Raman peak linewidth at 142 cm⁻¹ and 861 cm⁻¹ decreases, while the half peak width of the OH⁻ absorption spectrum at 3461 cm⁻¹ becomes narrower, both of which have quantitative relationships and can be used to determine the composition of LT crystals. The Raman peak at 278 cm⁻¹ is related to V_{Li} , while the Raman peak at 750 cm⁻¹ is related to the vibration of anti Ta_{Li}^{4+} ions. As the Li content increases, the peaks at 278 cm⁻¹ and 750 cm⁻¹ continue to decrease and eventually tend to disappear, representing a decrease in the number of intrinsic defects in the NSLT crystal. Hydrogen is an inevitable natural impurity in the growth process of LT crystals. In CLT crystals, H ions are prone to occupying V_{Li} and forming hydrogen defects. However, NSLT crystals do not have defects related to H ions due to the few defects in the crystal, and according to research, other impurity ions are prone to occupying V_{Li} before occupying other positions [17].

The composition of NSLT crystal is more uniform than CLT crystal, so NSLT crystal has a lower coercive field [18–20], higher photorefractive damage threshold [21] and greater electro-optic coefficient [22] and thermal conductivity [18].

It can be seen from Table 1 that the coercivity field of CLT crystal is more than 10-times larger than NSLT crystal. Low coercivity field requires lower electric field strength to conduct domain inversion [23], so the voltage used for domain inversion of NSLT crystal is lower. Wirp et al. [24] fitted the relationship between Li concentration and coercive field strength according to the formula. As shown in Figure 2, the coercive field and internal electric field of LT crystal decrease with the increase of Li content. The thermal conductivity of the NSLT crystal is about twice that of the CLT crystal. This is because the NSLT crystal

has fewer defects, which reduces the phonon scattering caused by lattice defects so as to reduce thermal conductivity. Because the reduction of lithium vacancies promotes thermal diffusion, the thermal diffusion coefficient of the NSLT crystal is about twice that of CLT crystal [25].

Table 1. Performance comparison of CLT crystal and NSLT crystal [14,18,19,24–26].

	Coercive Field (V/m)	Curie Temperature (°C)	Domain Shape	Sound Velocity (m/s)	Thermal Conductivity W/(m·K)	Thermal Diffusivity ($10^{-4} \text{ m}^2/\text{s}$)
CLT	21,100	603	triangle	3294	4.67	0.0156
NSLT	2000	693	hexagon		8.78	0.0288

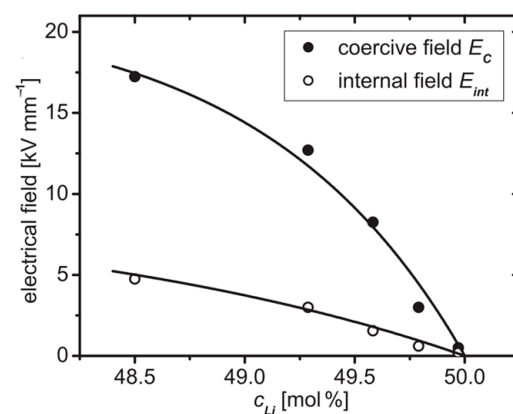


Figure 2. Changes of coercivity field and internal electric field of LT crystals with different Li concentrations fitted according to the formula [24].

In addition, after applying an electric field, the isolated domain shape of CLT crystal is triangular [27]. The domain wall is along the x -axis direction [2], while the domain wall of NSLT crystal is hexagonal [27]. The domain wall is along the y -axis direction, and the domain wall configuration is shown in Figure 3. It can be seen from the figure that with the increase of Li content, the domain wall shape will change from triangular to hexagonal. The hysteresis loops of CLT crystal and NSLT crystal are very different [28]. It can be seen from Figure 4 that the spontaneous polarization intensity of the CLT crystal changes more with the change of electric field. The change of spontaneous polarization intensity of NSLT crystal is smaller [2], which also proves that NSLT crystal has a smaller coercivity field than CLT crystal.

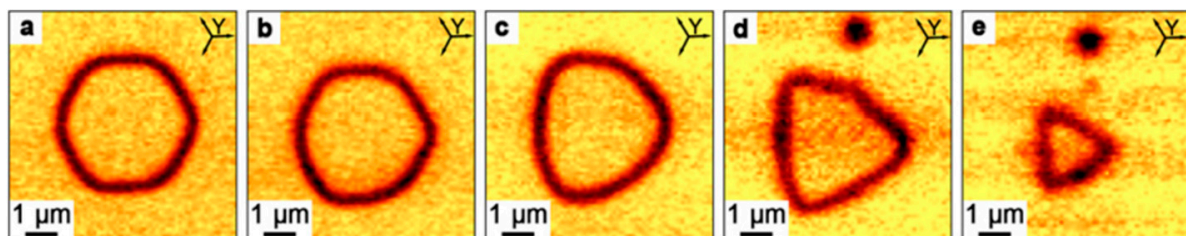


Figure 3. Domain structure of LT crystals with different Li contents: (a) 50%, (b) 49.9%, (c) 49.8%, (d) 49.4%, (e) 49.0% [27].

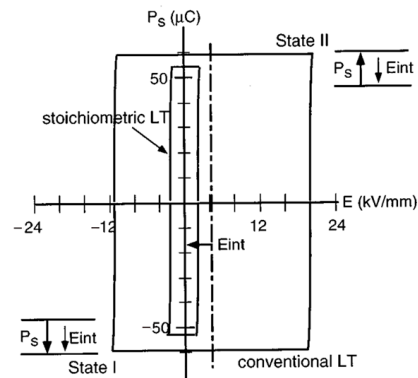


Figure 4. Hysteresis loops of CLT and SLT crystals [28].

The Curie temperature of LT crystal is closely related to the Li content [29]. It can be seen from Figure 5 that with the increase of Li content, the Curie temperature will increase. When the Li content is close to the stoichiometric ratio, the Curie temperature reaches 690 °C, and the increase of Curie temperature represents the decrease of defects in the crystal. Therefore, with the increase of Li content, the internal defects of LT crystal decrease. At the same time, the Li content is also related to the acoustic properties of LT crystal. The elastic constant of LT crystal increases with the increase of Li content, except for the elastic constant C_{44} , which decreases when it approaches the stoichiometric ratio [30]. Therefore, with the change of Li content, the surface acoustic wave propagation characteristics also change. For example, in the case of 33RY-XLT crystal cutting, by adding 1 mol% Li_2O [30], the speed of leaky surface acoustic wave (LSAW) increases by 23.8 m/s.

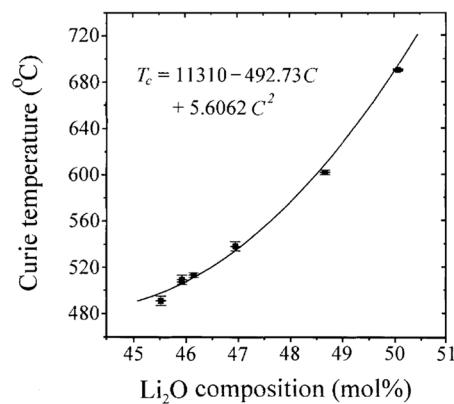


Figure 5. Relationship between Curie temperature and Li_2O mol% [29].

In conclusion, the NSLT crystal has fewer defects, smaller coercive field and larger thermal conductivity and thermal diffusion coefficient than the CLT crystal. Hence, the comprehensive performance of NSLT crystal is better than the CLT crystal.

3. Crystal Preparation Methods

At present, the main methods for preparing NSLT crystals are double crucible Czochralski method (DCCZ) [31], K_2O cosolvent method [32] and vapor transport equilibrium (VTE) method [33]. The VTE method can grow various components of LT crystals [34].

3.1. Double Crucible Czochralski Method

The DCCZ method is one of the most commonly used techniques for the preparation of NSLT crystals [31]. Kitamura et al. [28,35,36], of Japan, successfully prepared NSLT crystals by using the double crucible continuous packing technique and carried out periodic polarization research. In 1999, Furukawa et al. [37] grew colorless, transparent, and crack free NSLT crystals with a diameter of 45 mm and length of 80 mm by the DCCZ method, and

no mechanical twins were found. The advantage of this method is that the convection effect is reduced, and the service life of the crucible is prolonged due to the surface level of the melt during crystal growth. The grown NSLT crystal is shown in Figure 6. Kumaragurubaran et al. [38] used the DCCZ method to grow NSLT crystals with a diameter of four inches. They believed that the main problem in the growth of NSLT crystals by this method was that the instability of the temperature field led to the occurrence of cracks and twins.

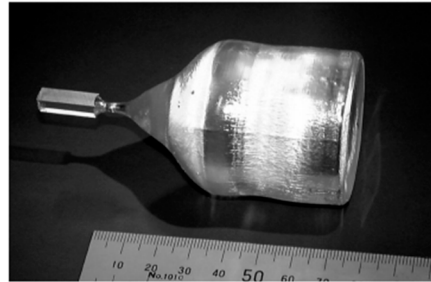


Figure 6. NSLT crystals grown by DCCZ method [37].

The equipment structure of DCCZ method is shown in Figure 7. The technology overcomes the problem of uneven composition of LT crystal grown by the Czochralski method. The DCCZ method has a smooth and continuous powder supply system [30], so that the whole crystal homogeneous doping and stoichiometric control can be realized. However, the DCCZ method has high equipment requirements and is a complex process, and it has the disadvantages of high production cost and difficulty in controlling the temperature field [39]; therefore, it is necessary to find other methods with less disadvantages and a simple process to prepare NSLT crystals.

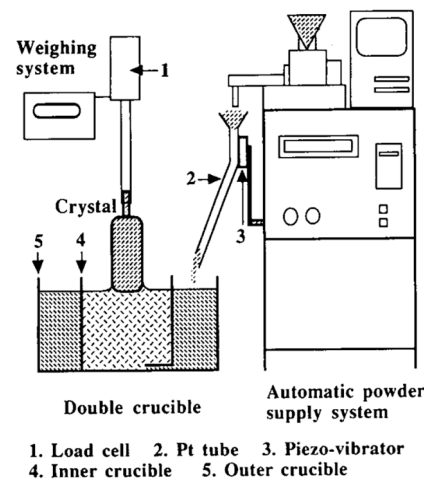


Figure 7. Schematic diagram of DCCZ method [31].

3.2. Cosolvent Method

The principle of the cosolvent method is to use a flux to reduce the melting point of LT crystals, thereby reducing the difficulty of NSLT crystal growth [39]. The specific steps are to produce LT polycrystalline powder using high-purity H_2TaF_7 and Li_2CO_3 through multiple processes, and then, convert it into LT crystal. Jia [32] and others prepared NSLT crystal by adding K_2O cosolvent. The crystal is shown in Figure 8. The Curie temperature of the prepared crystal is $673\text{ }^\circ\text{C}$, which indicates that the composition of the prepared crystal is close to near stoichiometric, and it can be expected to be applied in optics. The growth of NSLT crystals by the cosolvent method will inevitably introduce some impurities [40], which will lead to crystal impurity. Therefore, other methods are needed to grow relatively pure NSLT crystals.

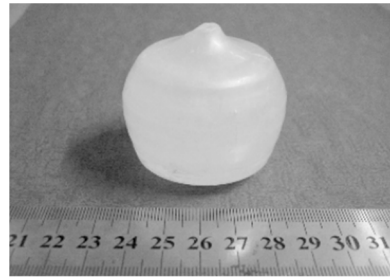


Figure 8. NSLT crystals prepared by cosolvent method [39].

3.3. Diffusion Method

An example of the experimental setup used in the diffusion method, also known as VTE method, is shown in Figure 9 [41]. During the treatment, the crystal composition changes due to the exchange of Li_2O .

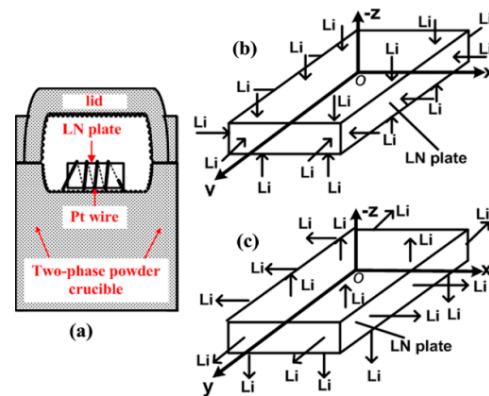


Figure 9. Schematic diagram of experimental device for VTE process (a) Li rich (b) Li poor (c) Schematic diagram of Li diffusion in VTE [41].

In 2018, Yang et al. [42] prepared NSLT crystals with a thickness of 3.1 mm and diameter of 56 mm by VTE method. The content of Li with different thicknesses were calculated by the Curie temperature method. The Curie temperature is shown in Figure 10. It was found that the Curie temperature is close to 694 °C, and the measured positive and negative polarization electric fields are 159 V/mm and 145 V/mm, respectively. The composition in the crystal is basically uniform.

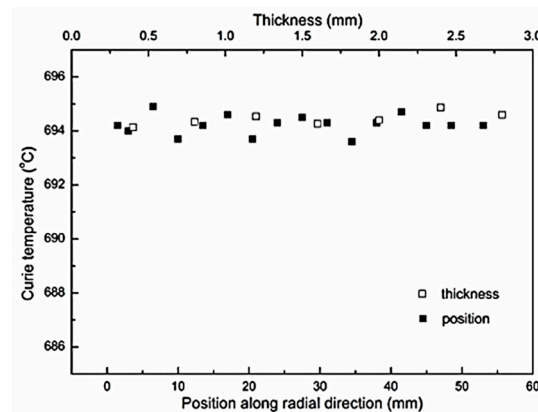


Figure 10. Curie temperature of NSLT at different depths [42].

Yang et al. [43] found that when the NSLT was grown by VTE method, the temperature had a great influence on the crystal structure and properties. Stoichiometric lithium tantalate (SLT) could not be grown at 1100 °C and the twin defects appeared when the

temperature was low. Meanwhile, the plane of the crystal was $\{01\bar{1}2\}$ plane and the appearance of twins would make the crystal crack. It was found that when the crystal was treated at 1350 °C for 250 h, the growth rate of SLT was higher. The Curie temperature of crystal growth is 693.8 °C. The NSLT crystals can be prepared by the VTE method, but there are also certain problems. The first problem is the thickness of the wafer. The NSLT crystals are very thin, about a few millimeters. It can be seen from Figure 10 that although the Curie temperatures of different thicknesses are close, there is still a difference of about 10 °C, which indicates that the uniformity of Li cannot be achieved.

In conclusion, the main methods for growing NSLT crystals include DCCZ method and VTE method. Each method has its advantages and disadvantages; as shown in Table 2, the DCCZ method can theoretically grow high-quality NSLT crystals, but it is expensive and process parameters are difficult to control. The VTE method has the advantages of simple operation process and low cost, and it is the best method to reduce the production cost of high-quality SAW filters. However, using VTE method to prepare NSLT wafers can easily lead to surface warping, twinning grain boundaries, and inability to control the Li content inside the wafers. Therefore, it is necessary to improve the VTE method preparation process in order to achieve mass production of high-quality NSLT wafers.

Table 2. Comparison of advantages and drawbacks of crystal preparation methods.

Preparation Method	Advantage	Drawback
DCCZ method	<ol style="list-style-type: none"> 1. Uniform doping of crystals 2. Stoichiometry can be controlled 	<ol style="list-style-type: none"> 1. Complex process 2. High production costs 3. The temperature field is difficult to control
Cosolvent method	<ol style="list-style-type: none"> 1. Crystal composition closer to stoichiometric ratio 	<ol style="list-style-type: none"> 1. Easy to introduce impurities
VTE method	<ol style="list-style-type: none"> 1. Simple operation process 2. Low production cost 	<ol style="list-style-type: none"> 1. Temperature has a significant impact on crystal structure 2. The crystal is very thin 3. Uneven distribution of Li ions

4. Application of Crystal in Optics

CLT crystals have many defects, and the Ta_{Li} antiposition defect is an important reason for the optical damage effect [7]. Therefore, the application of NSLT crystals with fewer defects to the optical field will improve the performance of optical devices and doped NSLT crystals can further improve the optical performance of crystals.

Kostritskii et al. [44] found through Raman spectroscopy and infrared reflection spectroscopy that the structure of NSLT crystal is a mixture of LT main structure and ilmenite-like structure, and this method can quickly determine the electro-optical and nonlinear optical coefficients of the crystal. The current problem is the uneven distribution of Li ions in NSLT crystals, but the composition of NSLT crystals prepared by VTE technology is almost uniform, which is expected to be used to produce NSLT crystals with uniform composition for integrated optical devices [45].

Kumaragurubaran et al. [35] studied the NSLT crystals doped with MgO of different concentrations. When the MgO concentration reaches 0.7%, the photorefractive damage resistance reaches 670 kw/cm², which is much higher than the undoped NSLT crystals. Nan et al. [46] measured the NSLT crystals doped with different concentrations of MgO and measured the Curie temperature and coercive field. It was concluded that the NSLT crystals doped with 1% MgO have good uniformity, which also reduces the photorefractive properties of the crystal itself. Stable Second Harmonic Generation can be achieved by periodically poling MgO doped in NSLT crystals, which can be used to fabricate optical parametric oscillators (OPO) [47–49]. At the same time, the NSLT crystal has good uniformity, recordability and erasability, which makes it one of the best materials for holographic memory.

4.1. Holographic Memory

The advantage of holographic memory is that it can write and erase information repeatedly, but the disadvantage is instability, i.e., an erasing operation may occur during writing and reading [50,51]. Hence, it is necessary to find more stable materials to make holographic memory. LT crystal has become one of the best choices for holographic storage materials because of its readability, erasure and good optical parameters [52–55]. LT crystal has a storage density of 10^{12} bits/cm³, a high transmission speed of 10^9 bits/s, a small proton mobility and has a longer dark storage time [56] than Fe-CLN crystal (1 year). CLT crystal has serious disadvantages, including long recording time, long erasing time and low optical efficiency [57]. At the same time, NSLT crystal also shows higher response speed and sensitivity [11].

Holographic storage technology uses a laser to change the refractive index to record information, and volatility is the change of refractive index with time. It can be seen from Figure 11 that the non-volatile property of NSLT is very good. After a long time, the refractive index change of the crystal is very small, while the non-volatile property of near stoichiometric lithium niobate (NSLN) and doped NSLN is very poor [58]. Liu et al. [58] studied the reading, writing and erasing process of NSLT holographic storage. The reading, writing and erasing process is shown in Figure 12. It is found that NSLT as a holographic storage material has the characteristics of high sensitivity and good non-volatile property, so NSLT is a potential holographic storage material.

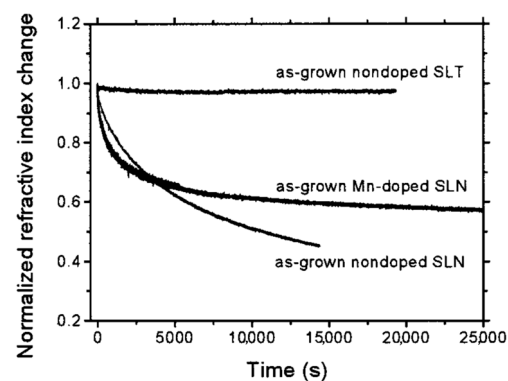


Figure 11. Comparison of nonvolatile readout of NSLT, NSLN and doped NSLN [58].

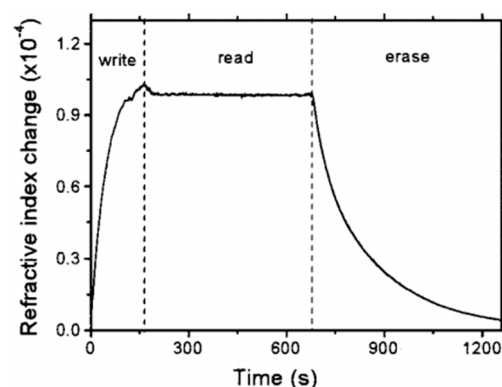


Figure 12. Refractive index change during reading, writing and erasing of NSLT crystal holographic storage, with writing energy of 11.2 W/cm^2 [58].

Hsu et al. [59] think that doping Fe and Mg in NSLT crystal can improve the photorefractive properties and has high sensitivity. The recording time and sensitivity decrease with the increase of light intensity, and the diffraction efficiency increases with the increase of light intensity. Therefore, NSLT crystal is one of the best choices as holographic storage materials.

4.2. Application of Nonlinear Optics

At present, the main applications of NSLT crystal in nonlinear optics are optical parametric oscillators and laser generators. Because NSLT crystal has lower coercive field than CLT crystal, it is more suitable for making periodic polarization devices. Nan et al. [46] fabricated a 35 mm long optical oscillator with NSLT crystal. The maximum conversion efficiency is 65%. As shown in Figure 13, when the input power is 1 W, the output power is 600 mW. Rautiainen et al. [60] used the NSLT crystal to double the frequency in the cavity of a semiconductor laser and found that the second harmonic of 610 nm can be generated. The output power can reach 730 mW. Li et al. [61] used waveguide by direct femtosecond laser writing and a tunable titanium sapphire laser source. By adjusting the temperature of MgO doped periodically polarized NSLT crystals from 60 °C to 200 °C, they were able to tune and generate ultraviolet light in the range of 396–401 nm. Antsygin et al. [62] studied the influence of low temperature on the birefringence and ultraviolet absorption edge of NSLT. The research showed that with the cooling of the crystal, the ultraviolet absorption blue shifted by 8 nm at 1 THz, and its birefringence became larger, reducing the difficulty of Quasi-phase-matching. Rowley et al. [63] achieved broadly tunable in near-infrared (900–1350 nm) using an OPO based on periodically polarized NSLT crystals, with an average power of up to 150 mW at a repetition frequency of 532.3 MHz. Lee et al. [64] obtained a high-purity source of correlated photon pair at 711 nm using periodically polarized MgO doped NSLT crystals under a 355.7 nm pump laser.

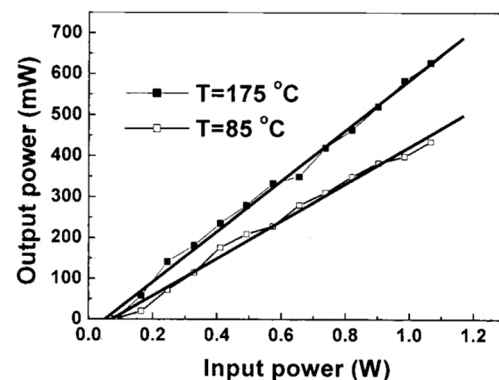


Figure 13. Output power corresponding to input power of optical resonator at different temperatures [46].

NSLT crystal has great potential in holographic memory devices and nonlinear optics, especially in making holographic memory. Therefore, further research on the optical properties of NSLT crystal and its use in holographic storage technology can realize the storage technology with larger internal memory and faster reading speed, which is expected to realize the reform of storage technology.

5. Application of Crystal in Radio Frequency SAW Filter

LT crystal is famous for low acoustic loss, high piezoelectric coupling coefficient and electro–optic properties. Therefore, this material is widely used in the manufacture of SAW filters. At present, 70% of radio frequency SAW filters are made of LT and LN single crystals. Radio frequency filters are generally used at frequencies below 2.5 GHz, while the frequency range of SAW filters used in mobile phones is 800 MHz to 2.5 GHz. The function of a SAW filter is to filter out clutter in other frequency bands. A communication frequency band needs several SAW filters. There are 5 communication frequency bands in 3G network and nearly 40 communication frequency bands in 4G network [64]. In the 5G era, there will be more than 60 communication frequency bands. Therefore, communication equipment needs more and more SAW filters. There are more and more requirements for SAW filters, including smaller size, better performance, wider frequency band and lower loss. At present, the best way to reduce the volume of a SAW filter is wafer level packaging

(WLP) technology. Of course, to realize the application, we need to reduce the TCF. If the TCF is too high, a frequency shift of the equipment will occur [65].

In recent years, 5G technology is gradually maturing and 5G communication equipment has been initially developed. With the improvement of 5G communication equipment, it will face more and more clutter. Therefore, there are greater requirements for the volume and performance of SAW filters, including TCF and service life. The result of research has shown that the small diplexer based on LT structure has a longer lifetime [41].

The elastic wave propagating along the surface of an object is called surface acoustic wave. The propagation characteristics of SAW are mainly determined by the following parameters, including wave velocity, K^2 of piezoelectric substrate, quality factor (Q) and TCF [66]. The K^2 represents the conversion efficiency between electrical energy and mechanical energy, which mainly depends on the piezoelectric properties of materials, cutting or crystal orientation, and the type of propagating wave. The Q represents the loss of the circuit which is the average contrast ratio of the energy stored, and the power consumed in an operational cycle [66]. TCF represents the thermal stability of frequency and TCF depends on the elasticity, piezoelectric constant and dielectric constant of the piezoelectric substrate [67]. These parameters related to SAW filters are related to the performance of the piezoelectric substrate, so improving the performance of the piezoelectric substrate is very important to improve the performance of SAW filters.

It can be seen from Figure 14 that [67] the K^2 of multi domain NSLT crystal is higher than that of the single domain CLT crystal, and the K^2 reaches the maximum when Li:Ta = 1:1. It can be seen from Figure 15 that the sound velocity increases with the increase of Li content.

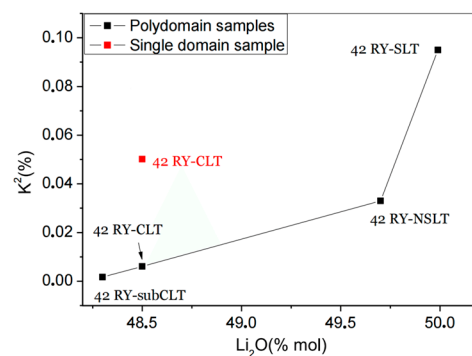


Figure 14. Evolution of K^2 and Li_2O in multi domain and single domain crystals with different Li nonstoichiometric ratios [68].

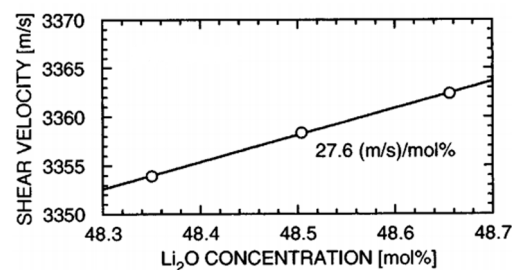


Figure 15. Relationship between sound velocity and Li content [30].

In conclusion, LT crystal is suitable for making filters and the K^2 of NSLT crystal is larger than CLT crystal. The defects of NSLT crystal are less than CLT crystal, and the performance of NSLT crystal is better than CLT crystal. If the NSLT crystal is used in the fabrication of SAW filters, it is expected to improve the performance of the filter itself by reducing the TCF and realizing the application of SAW filters in 5G communication.

6. Expectation

LT crystals are widely used in optical and acoustic fields because of excellent piezoelectric, pyroelectric and nonlinear optical properties. The NSLT crystal has less defects and better performance than the CLT crystal, so it is expected to replace the CLT crystal in some fields. In order to realize the application of NSLT crystal in acoustics and optics, we should continue to strengthen the research in the following aspects.

The growth of large size and high quality NSLT crystals is a problem. Large size NSLT crystals can be grown by the DCCZ method. The quality of the crystals are excellent, but there are some problems, such as complex equipment, unstable temperature field and additionally, they are easy to crack. The properties of NSLT crystals prepared by the cosolvent method are better than CLT crystals, but impurity ions are introduced. Although the VTE method has a simple process, low cost and can prepare high-quality NSLT wafers, it has poor repeatability, and the prepared wafers are prone to problems such as uneven distribution of Li ions, twinning and cracking. Therefore, a new method is needed to grow NSLT crystals. After multiple theoretical and experimental studies, our research group has proposed using guided mode method [69] to grow NSLT crystals, which can solve problems such as component segregation and small crystal volume growth. Further study of the growth of NSLT crystals by the guided mode method is required.

To explore and strengthen the application of NSLT crystals in sound and light. The research of NSLT crystal focuses on the optical application, but neglects the acoustic research, including some physical parameters, such as TCF, etc. The performance of NSLT crystal is better than CLT crystal. Whether the performance of SAW filters can be improved by using NSLT crystal instead of the CLT crystal, and then, be directly applied to 5G communication equipment, is a research direction. In addition, the CLT crystal can reduce the pyroelectric effect in the chip through reduction treatment [70], reduce the damage of devices caused by the accumulated charge due to heating and reduce the transmittance. The reduced NSLT crystal sheet can be directly applied to the fabrication of SAW filters; whether the performance of SAW filters can be improved is also a research focus. At present, it is known that cooling can improve the birefringence of crystals, but no one has studied the specific mechanism of the influence of defect concentration on birefringence, including the mechanism of the influence on the ultraviolet absorption edge. This is also one of the main reasons why NSLT crystals have not been truly applied in optics.

Author Contributions: All authors contributed to the study conception and design. The organization of the final data and the first draft of the manuscript was written by X.X. and J.S. S.L. mainly collected and organized data on crystal physical properties. The summary of data on crystal growth is the responsibility of Q.X. and H.Z. L.M. and C.Y. collected the information on optical applications. X.Z.'s main contribution is in the field of SAW filters, and all authors commented on previous versions of the manuscript. All authors have read and agreed to the published version of the manuscript.

Funding: This work is supported by the National Natural Science Foundation of China (61965001 11864001 and 61461001), the Fundamental Research Funds for the Central Universities, North Minzu University (2020DXXY002 and 2021KJCX07), the Ningxia Province Key Research and Development Program (2018BEE03015 and 2021BEE03005), the Ningxia key Natural Science Foundation project (2023AAC02045) and the Natural Science Foundation of Ningxia (2019AAC03103 and 2020AAC03239), the Ningxia first-class discipline and scientific research projects (electronic science and technology, No. NXYLXK2017A07-DKPD2023C10 and DKPD2023D01).

Data Availability Statement: The data pertaining to this report can be provided on reasonable request.

Acknowledgments: The authors thank the Key Laboratory of North Minzu University (Physics and Photoelectric Information Functional Materials Sciences and Technology), the Ningxia advanced intelligent perception control innovation team, the Ningxia acoustooptic-crystals industrialization Innovation team and the Ningxia new solid electronic materials and Devices research and development innovation team (2020CXTDLX12).

Conflicts of Interest: The authors declare no conflict of interest.

References

1. Imbrock, J.; Wevering, S.; Buse, K.; Krätzig, E. Nonvolatile holographic storage in photorefractive lithium tantalate crystals with laser pulses. *JOSA B* **1999**, *16*, 1392–1397. [[CrossRef](#)]
2. Hatanaka, T.; Nakamura, K.; Taniuchi, T.; Ito, H.; Furukawa, Y.; Kitamura, K. Quasi-phase-matched optical parametric oscillation with periodically poled stoichiometric LiTaO₃. *Opt. Lett.* **2000**, *25*, 651–653. [[CrossRef](#)] [[PubMed](#)]
3. Porter, S. A brief guide to pyroelectric detectors. *Ferroelectrics* **1981**, *33*, 193–206. [[CrossRef](#)]
4. Lerner, P.; Legras, C.; Dumas, J. Stoechiométrie des monocristaux de métaniobate de lithium. *J. Cryst. Growth* **1968**, *3*, 231–235. [[CrossRef](#)]
5. Abrahams, S.; Marsh, P. Defect structure dependence on composition in lithium niobate. *Acta Crystallogr. Sect. B Struct. Sci.* **1986**, *42*, 61–68. [[CrossRef](#)]
6. Palatnikov, M.; Shcherbina, O.; Sandler, V.; Sidorov, N.; Bormanis, K. Effects of VTE treatment on composition of lithium tantalate single crystals. *Ferroelectrics* **2011**, *417*, 46–52. [[CrossRef](#)]
7. Imbrock, J.; Kip, D.; Krätzig, E. Nonvolatile holographic storage in iron-doped lithium tantalate with continuous-wave laser light. *Opt. Lett.* **1999**, *24*, 1302–1304. [[CrossRef](#)]
8. He, C.; Li, W.; Wang, J. Growth and optical properties of indium neodymium doped lithium tantalate single crystals. *Acta Opt. Sin.* **2018**, *38*, 0116003.
9. Katz, M.; Route, R.K.; Hum, D.S.; Parameswaran, K.R.; Miller, G.D.; Fejer, M.M. Vapor-transport equilibrated near-stoichiometric lithium tantalate for frequency-conversion applications. *Opt. Lett.* **2004**, *29*, 1775–1777. [[CrossRef](#)]
10. Hum, D.S.; Route, R.K.; Miller, G.D.; Kondilenko, V.; Alexandrovski, A.; Huang, J.; Urbanrk, K.; Byer, R.L.; Fejer, M.M. Optical properties and ferroelectric engineering of vapor-transport-equilibrated, near-stoichiometric lithium tantalate for frequency conversion. *J. Appl. Phys.* **2007**, *101*, 093108. [[CrossRef](#)]
11. Furukawa, Y.; Kitamura, K.; Hatano, K.; Bernasconi, P.; Montemezzani, G.; Günter, P. Stoichiometric LiTaO₃ for dynamic holography in near UV wavelength range. *JPN J. Appl. Phys.* **1999**, *38*, 1816. [[CrossRef](#)]
12. Meyn, J.P.; Fejer, M. Tunable ultraviolet radiation by second-harmonic generation in periodically poled lithium tantalate. *Opt. Lett.* **1997**, *22*, 1214–1216. [[CrossRef](#)] [[PubMed](#)]
13. Sánchez-dena, O.; Villalobos-mendoza, S.D.; Farías, R.; Fierro-Ruiz, C.D. Lithium niobate single crystals and powders reviewed—Part II. *Crystals* **2020**, *10*, 990. [[CrossRef](#)]
14. Katz, M.; Blau, P.; Shulga, B. Room Temperature High Power Frequency Conversion in Periodically Poled Quasi-Phase-Matched Crystals. In *Nonlinear Frequency Generation and Conversion: Materials, Devices, and Applications VII*; SPIE: Bellingham, WA, USA, 2008; Volume 6875, pp. 18–31.
15. Shi, L.; Kong, Y.; Yan, W.; Liu, H.; Li, X.; Xie, X.; Zhao, D.; Sun, L.; Xu, J.; Sun, J. The composition dependence and new assignment of the Raman spectrum in lithium tantalate. *Solid State Commun.* **2005**, *135*, 251–256. [[CrossRef](#)]
16. Shi, L.; Kong, Y.; Yan, W.; Sun, J.; Chen, S.; Zhang, L.; Zhang, W.; Liu, H.; Li, X.; Xie, X. Determination of the composition of lithium tantalate by means of Raman and OH[−] absorption measurements. *Mater. Chem. Phys.* **2006**, *95*, 229–234. [[CrossRef](#)]
17. Köhler, T.; Zschornak, M.; Röder, C.; Hanzig, J.; Gärtner, G.; Leisegang, T.; Meyer, D.C. Chemical environment and occupation sites of hydrogen in LiMO₃. *J. Mater. Chem. C* **2023**, *11*, 520–538. [[CrossRef](#)]
18. Kitamura, K.; Takekawa, S.; Nakamura, M.; Kurimura, S.; Louchev, O. Defect density dependence of thermal conductivity and temperature control of quasi-phases matching devices. In *Conference on Lasers and Electro-Optics*; Optical Society of America: Baltimore, MD, USA, 2005; pp. 22–27.
19. Tian, L.; Gopalan, V.; Galambos, L. Domain reversal in stoichiometric LiTaO₃ prepared by vapor transport equilibration. *Appl. Phys. Lett.* **2004**, *85*, 4445–4447. [[CrossRef](#)]
20. Kitamura, K.; Furukawa, Y.; Takekawa, S.; Hatanaka, T.; Ito, H.; Gopalan, V. Non-stoichiometric control of LiNbO₃ and LiTaO₃ in ferroelectric domain engineering for optical devices. *Ferroelectrics* **2001**, *257*, 235–243. [[CrossRef](#)]
21. Hsu, W.T.; Chen, Z.B.; You, C.A.; Chou, M.M.; Lin, Y.Y.; Huang, Y.C.; Rai, D.K.; Lan, C.W. Zone-leveling Czochralski growth and characterization of undoped and MgO-doped near-stoichiometric lithium tantalate crystals. *J. Cryst. Growth* **2008**, *311*, 66–71. [[CrossRef](#)]
22. Juvalta, F.; Jazbinsek, M.; Günter, P.; Kitamura, K. Electro-optical properties of near-stoichiometric and congruent lithium tantalate at ultraviolet wavelengths. *JOSA B* **2006**, *23*, 276–281. [[CrossRef](#)]
23. Gopalan, V.; Mitchell, T.E.; Furukawa, Y.; Kitamura, K. The role of nonstoichiometry in 180 domain switching of LiNbO₃ crystals. *Appl. Phys. Lett.* **1998**, *72*, 1981–1983. [[CrossRef](#)]
24. Wirp, A.; Bäumer, C.; Hesse, H.; Kip, D.; Krätzig, E. Magnesium-doped near-stoichiometric lithium tantalate crystals for nonlinear optics. *Phys. Status Solid A* **2005**, *202*, 1120–1123. [[CrossRef](#)]
25. Birnie, D.P., III; Bordui, P.F. Defect-based description of lithium diffusion into lithium niobate. *J. Appl. Phys.* **1994**, *76*, 3422–3428. [[CrossRef](#)]
26. Song, L.; Li, M.; Xu, Y. Study on the Growth and Physical Properties of lithium tantalate Crystal. *J. Synth. Cryst.* **1994**, *23*, 146–150.
27. Pryakhina, V.I.; Greshnyakov, E.D.; Lisjikh, B.I.; Nebogatikov, M.S.; Shur, V.Y. Influence of composition gradients on heat induced initial domain structure in lithium tantalate. *Ferroelectrics* **2019**, *542*, 13–20. [[CrossRef](#)]
28. Kitamura, K.; Furukawa, Y.; Niwa, K.; Gopalan, V.; Mitchell, T.E. Crystal growth and low coercive field 180° domain switching characteristics of stoichiometric LiTaO₃. *Appl. Phys. Lett.* **1998**, *73*, 3073–3075. [[CrossRef](#)]

29. Kim, I.G.; Takekawa, S.; Furukawa, Y.; Lee, M.; Kitamura, K. Growth of $\text{Li}_x\text{Ta}_{1-x}\text{O}_3$ single crystals and their optical properties. *J. Cryst. Growth* **2001**, *229*, 243–247. [[CrossRef](#)]
30. Kushibiki, J.; Takanaga, I.; Komatsuzaki, S.; Ujiie, T. Chemical composition dependences of the acoustical physical constants of LiNbO_3 and LiTaO_3 single crystals. *J. Appl. Phys.* **2002**, *91*, 6341–6349. [[CrossRef](#)]
31. Kitamura, K.; Yamamoto, J.K.; Iyi, N.; Kirnura, S.; Hayashi, T. Stoichiometric LiNbO_3 single crystal growth by double crucible Czochralski method using automatic powder supply system. *J. Cryst. Growth* **1992**, *116*, 327–332. [[CrossRef](#)]
32. Jia, B.; Zhao, Y. Near stoichiometric lithium tantalate crystal growth and its periodic polarization. *Acta Opt. Sin.* **2010**, *30*, 3249–3252.
33. Bordui, P.F.; Norwood, R.G.; Bird, C.D.; Carella, J.T. Stoichiometry issues in single-crystal lithium tantalate. *J. Appl. Phys.* **1995**, *78*, 4647–4650. [[CrossRef](#)]
34. Holtmann, F.; Imbrock, J.; Bäumer, C.; Hesse, H.; Krätzig, E.; Kip, D. Photorefractive properties of undoped lithium tantalate crystals for various composition. *J. Appl. Phys.* **2004**, *96*, 7455–7459. [[CrossRef](#)]
35. Kumaragurubaran, S.; Takekawa, S.; Nakamura, M.; Kitamura, K. Growth of 4-in diameter MgO-doped near-stoichiometric lithium tantalate single crystals and fabrication of periodically poled structures. *J. Cryst. Growth* **2006**, *292*, 332–336. [[CrossRef](#)]
36. Ganesamoorthy, S.; Nakamura, M.; Takekawa, S.; Kumaragurubaran, S.; Terabe, K.; Kitamura, K. A comparative study on the domain switching characteristics of near stoichiometric lithium niobate and lithium tantalate single crystals. *Mater. Sci. Eng. B* **2005**, *120*, 125–129. [[CrossRef](#)]
37. Furukawa, Y.; Kitamura, K.; Suzuki, E.; Niwa, K. Stoichiometric LiTaO_3 single crystal growth by double crucible Czochralski method using automatic powder supply system. *J. Cryst. Growth* **1999**, *197*, 889–895. [[CrossRef](#)]
38. Kumaragurubaran, S.; Takekawa, S.; Nakamura, M.; Kitamura, K. Growth of 4-in diameter near-stoichiometric lithium tantalate single crystals. *J. Cryst. Growth* **2005**, *285*, 88–95. [[CrossRef](#)]
39. Zhang, X.; Qiao, W.; Liu, J. Growth and characterization of near stoichiometric lithium tantalate crystals. *Rare Metals Lett.* **2007**, *26*, 23–26.
40. Su, D.; Liu, H.; Yan, T. Near stoichiometric lithium tantalate crystals-growth techniques and composition testing methods. *J. Synth. Cryst.* **2011**, *40*, 528–572.
41. Zhang, D.L.; Chen, B.; Yu, D.Y.; Pun, E.Y.B. Influence of factors on growth of off-congruent LiNbO_3 single-crystal by li-rich/li-poor chemical vapor transport equilibration. *Cryst. Growth Des.* **2013**, *13*, 1793–1798. [[CrossRef](#)]
42. Yang, J.; Mao, Q.; Shang, J.; Hao, H.; Li, Q.; Huang, C.; Zhang, L.; Sun, J. Preparation and characterization of thick stoichiometric lithium tantalate crystals by vapor transport equilibration method. *Mater. Lett.* **2018**, *232*, 150–152. [[CrossRef](#)]
43. Yang, J.; Sun, J.; Xu, J.; Li, Q.; Shang, J.; Zhang, L.; Liu, S.; Huang, C. Twin defects in thick stoichiometric lithium tantalate crystals prepared by a vapor transport equilibration method. *J. Cryst. Growth* **2016**, *433*, 31–35. [[CrossRef](#)]
44. Kostritskii, S.M.; Bourson, P.; Aillierie, M.; Fontana, M.; Kip, D. Quantitative evaluation of the electro-optic effect and second-order optical nonlinearity of lithium tantalate crystals of different compositions using Raman and infrared spectroscopy. *Appl. Phys. B* **2006**, *82*, 423–430. [[CrossRef](#)]
45. Kostritskii, S.M.; Aillierie, M.; Bourson, P.; Kip, D. Raman spectroscopy study of compositional inhomogeneity in lithium tantalate crystals. *Appl. Phys. B* **2009**, *95*, 125–130. [[CrossRef](#)]
46. Yu, N.E.; Kurimura, S.; Nomura, Y.; Nakamura, M.; Kitamura, K.; Sakuma, J.; Otani, Y.; Shiratori, A. Periodically poled near-stoichiometric lithium tantalate for optical parametric oscillation. *Appl. Phys. Lett.* **2004**, *84*, 1662–1664. [[CrossRef](#)]
47. Yu, N.E.; Kurimura, S.; Nomura, Y.; Kitamura, K. Stable high-power green light generation with thermally conductive periodically poled stoichiometric lithium tantalate. *JPN J. Appl. Phys.* **2004**, *43*, L1265. [[CrossRef](#)]
48. Yu, N.E.; Kurimura, S.; Nakamura, M.; Nomura, Y.; Kitamura, K.; Sakuma, J.; Shiratori, A. Periodically Poled Stoichiometric LiTaO_3 for Optical Parametric Oscillation. In *Conference on Lasers and Electro-Optics*; Optica Publishing Group: Washington, DC, USA, 2003.
49. Getman, A.G.; Popov, S.V.; Taylor, J.R. 7 W average power, high-beam-quality green generation in MgO-doped stoichiometric periodically poled lithium tantalate. *Appl. Phys. Lett.* **2004**, *85*, 3026–3028. [[CrossRef](#)]
50. Psaltis, D.; Burr, G.W. Holographic data storage. *Computer* **1998**, *31*, 52–60. [[CrossRef](#)]
51. Barbastathis, G.; Psaltis, D. Volume holographic multiplexing methods. *Hologr. Data Storage* **2000**, *76*, 21–62.
52. Steinberg, I.S.; Shepetkin, Y.A. Two-photon recording of microholograms in undoped lithium tantalate. *Appl. Opt.* **2008**, *47*, 9–14. [[CrossRef](#)] [[PubMed](#)]
53. Wang, K.M.; Hu, H.; Chen, F.; Lu, F.; Zhang, J.H.; Liu, X.D.; Liu, J.T.; Shi, B.R. Damage profile and mode observation in LiTaO_3 by low-energy H^+ ions. *Can. J. Phys.* **2001**, *79*, 921–927. [[CrossRef](#)]
54. Krätzig, E.; Buse, K. Two-Step processes and IR recording in photorefractive crystals. In *Infrared Holography for Optical Communications: Techniques, Materials, and Devices*; Springer: Berlin/Heidelberg, Germany, 2002; pp. 23–40.
55. Bai, Y.; Neurgaonkar, R.; Kachru, R. High-efficiency nonvolatile holographic storage with two-step recording in praseodymium-doped lithium niobate by use of continuous-wave lasers. *Opt. Lett.* **1997**, *22*, 334–336. [[CrossRef](#)] [[PubMed](#)]
56. Krätzig, E.; Orłowski, R. LiTaO_3 as holographic storage material. *Appl. Phys.* **1978**, *15*, 133–139. [[CrossRef](#)]
57. Nakamura, M.; Takekawa, S.; Terabe, K.; Kitamura, K.; Usami, T.; Nakamura, K.; Ito, H.; Furukawa, Y. Near-stoichiometric LiTaO_3 for bulk quasi-phase-matched devices. *Ferroelectrics* **2002**, *273*, 199–204. [[CrossRef](#)]

58. Liu, Y.; Kitamura, K.; Takekawa, S.; Nakamura, M.; Furukawa, Y.; Hatano, H. Nonvolatile two-color holographic recording in nondoped near-stoichiometric lithium tantalate crystals with continuous-wave lasers. *Appl. Phys. Lett.* **2003**, *82*, 4218–4220. [[CrossRef](#)]
59. Hsu, W.T.; Chen, Z.B.; You, C.A.; Huang, S.W.; Liu, J.P.; Lan, C.W. Growth and photorefractive properties of Mg, Fe co-doped near-stoichiometric lithium tantalate single crystals. *Opt. Mater.* **2010**, *32*, 1071–1076. [[CrossRef](#)]
60. Rautiainen, J.; Okhotnikov, O.G.; Eger, D.; Zolotovskaya, S.A.; Fedorova, K.A.; Rafailov, E.U. Intracavity generation of 610 nm light by periodically poled near-stoichiometric lithium tantalate. *Electron. Lett.* **2009**, *45*, 1. [[CrossRef](#)]
61. Li, L.; Zhang, B.; Romero, C.; de Aldana, J.R.V.; Wang, L.; Chen, F. Tunable violet radiation in a quasi-phase-matched periodically poled stoichiometric lithium tantalate waveguide by direct femtosecond laser writing. *Results Phys.* **2020**, *19*, 103373. [[CrossRef](#)]
62. Antsygin, V.D.; Mamrashev, A.A.; Maximov, L.V.; Mikerin, S.L.; Minakov, F.A.; Nikolaev, N.A. Temperature Dependence of Terahertz Properties of Stoichiometric Lithium Tantalate. *J. Infrared Millim. Terahertz Waves* **2022**, *43*, 1–10. [[CrossRef](#)]
63. Rowley, J.D.; Yang, S.; Ganikhanov, F. Power and tuning characteristics of a broadly tunable femtosecond optical parametric oscillator based on periodically poled stoichiometric lithium tantalate. *JOSA B* **2011**, *28*, 1026–1036. [[CrossRef](#)]
64. Lee, H.J.; Kim, H.; Cha, M.; Moon, H.S. Generation of bright visible photon pairs using a periodically poled stoichiometric lithium tantalate crystal. *Opt. Express* **2015**, *23*, 14203–14210. [[CrossRef](#)]
65. Warder, P.; Layus, N. Selecting filters for challenging mobile applications worldwide. *Microw. J.* **2013**, *56*, 96.
66. Campbell, C. Surface acoustic wave devices and their signal processing applications. *J. Acoust. Soc. Am.* **1991**, *89*, 1479–1480. [[CrossRef](#)]
67. Dvoesherstov, M.Y.; Petrov, S.G.; Cherednik, V.I.; Chirimanov, A.P. The temperature coefficients of delay of surface acoustic waves in LGS and LGN crystals in a wide temperature range. *Tech. Phys.* **2001**, *46*, 346–347. [[CrossRef](#)]
68. Gonzalez, M. Impact of Li Non-Stoichiometry on the Performance of Acoustic Devices on LiTaO₃ and LiNbO₃ Single Crystals. Ph.D. Thesis, Université de Franche-Comté, Besançon, France, 2016.
69. Xiao, X.; Zhang, X.; Zhang, H.; Lei, Y.; Ma, T.; Wei, H.; Wei, T.; Zhang, S.; Li, W. Method of (Near) Stoichiometric Lithium Tantalate (LiTaO₃) Crystal Growth by the Edge Defined Film Fed Growth (EFG). Method. Patent CN111549374A, 18 August 2020.
70. Xiao, X.; Xu, Q.; Liang, S.; Zhang, H.; Ma, L.; Hai, L.; Zhang, X. Preparation, electrical, thermal and mechanical properties of black lithium tantalate crystal wafers. *J. Mater. Sci. Mater. Electron.* **2020**, *31*, 16414–16419. [[CrossRef](#)]

Disclaimer/Publisher's Note: The statements, opinions and data contained in all publications are solely those of the individual author(s) and contributor(s) and not of MDPI and/or the editor(s). MDPI and/or the editor(s) disclaim responsibility for any injury to people or property resulting from any ideas, methods, instructions or products referred to in the content.